PHYSICAL REVIEW D **87,** 074039 (2013)

Production of $c\bar{c}c\bar{c}$ in double-parton scattering within the k_t-factorization approach: Meson-meson correlations

Rafał Maciuła*
Institute of Nuclear Physics PAN, PL-31-342 Cracow, Poland

Antoni Szczurek†
Institute of Nuclear Physics PAN, PL-31-342 Cracow, Poland and University of Rzeszów, PL-35-959 Rzeszów, Poland
(Received 29 January 2013; published 30 April 2013)

We discuss production of two pairs of $c\bar{c}$ in proton-proton collisions at the LHC. Both double-parton scattering (DPS) and single-parton scattering contributions are included in the analysis. Each step of DPS is calculated within a k_t-factorization approach, which effectively includes some next-to-leading-order corrections. The conditions of how to identify the DPS contribution are presented. The discussed mechanism unavoidably leads to the production of pairs of mesons: D_iD_j (each containing c quarks) or $\bar{D}_i\bar{D}_j$ (each containing $\bar{c}$ antiquarks). We calculate corresponding production rates for different combinations of charmed mesons as well as some differential distribution for $(D^0D^0 + \bar{D}^0\bar{D}^0)$ production. Within large theoretical uncertainties, the predicted DPS cross section is fairly similar to the cross section measured recently by the LHCb collaboration. The best description is obtained with the Kimber-Martin-Ryskin unintegrated gluon distribution, which very well simulates higher-order corrections. The contribution of single-parton scattering, calculated in the high-energy approximation, turned out to be rather small. Finally, we emphasize the significant contribution of the DPS mechanism to inclusive charmed meson spectra measured recently by ALICE, ATLAS, and the LHCb.

DOI: 10.1103/PhysRevD.87.074039 PACS numbers: 13.87.Ce, 14.65.Dw

I. INTRODUCTION

There has been recently renewed interest in studying double-parton scattering (DPS) effects in different reactions (see, e.g., Ref. [1] and references therein). Very recently, we have shown that the production of $c\bar{c}c\bar{c}$ is a very good place to study DPS effects [2]. Here, the quark mass is small enough to assure that the cross section for DPS is very large and large enough that each of the scatterings can be treated within perturbative QCD. The calculations performed in Ref. [2] were done in the leading-order (LO) collinear approximation. This may not be sufficient when comparing the results of the calculation with real experimental data. In the meantime, the LHCb Collaboration presented new interesting data for simultaneous production of two charmed mesons [3]. The collaboration has observed a large percentage of the events with two mesons, both containing the c quark, with respect to the typical production of the corresponding meson/antimeson pair ($\sigma_{D_iD_j}/\sigma_{D_i\bar{D}_j} \sim 10\%$), despite the very limited LHCb acceptance.

Is the large effect a footprint of double-parton scattering? We wish to address the issue in this paper. In addition, we shall estimate $c\bar{c}c\bar{c}$ production via single-parton scattering (SPS) within a high-energy approximation [4]. This approach should be an efficient tool especially when the distance in rapidity between cc or/and $\bar{c}\,\bar{c}$ is large.

Another piece of evidence for the DPS effects is that their absence leads to a missing contribution to inclusive charmed meson production, as noted in Ref. [5]. The measured inclusive cross sections include events where two D (or two $\bar{D}$) mesons are produced; therefore, corresponding theoretical predictions should also be corrected for the DPS effects.

In Ref. [6], the authors estimated DPS contribution based on the experimental inclusive D meson spectra measured at LHC. In their approach, fragmentation was included only in terms of the branching fractions for the transition $c \to D$. In our approach, we shall include full kinematics of the hadronization process. Here, we wish to also show first differential distributions on the hadron level to be confronted with recent LHCb experimental data [3].

II. THEORETICAL FRAMEWORK

In the present analysis, when considering the $pp \to c\bar{c}c\bar{c}X$ reaction, we concentrate primarily on double-parton scattering effects. In Sec. III B, we will show that the single-scattering contribution to double-charm production is much smaller, especially in the LHCb kinematics.

A. Double-parton scattering

In the LO collinear approximation, the differential distributions for $c\bar{c}$ production depend, e.g., on rapidity of the quark, rapidity of the antiquark, and transverse momentum of one of them (they are identical) [2]. In the next-to-leading order (NLO) collinear approach or in the

*rafal.maciula@ifj.edu.pl
†antoni.szczurek@ifj.edu.pl

k_t-factorization approach, the situation is more complicated as there are more kinematical variables necessary to describe the kinematical situation. In the k_t-factorization approach, the differential cross section for DPS production of the $c\bar{c}c\bar{c}$ system, assuming factorization of the DPS model, can be written as

$$\frac{d\sigma^{\rm DPS}(pp \to c\bar{c}c\bar{c}X)}{dy_1 dy_2 d^2p_{1,t} d^2p_{2,t} dy_3 dy_4 d^2p_{3,t} d^2p_{4,t}} = \frac{1}{2\sigma_{\rm eff}} \cdot \frac{d\sigma^{\rm SPS}(pp \to c\bar{c}X_1)}{dy_1 dy_2 d^2p_{1,t} d^2p_{2,t}} \cdot \frac{d\sigma^{\rm SPS}(pp \to c\bar{c}X_2)}{dy_3 dy_4 d^2p_{3,t} d^2p_{4,t}}. \tag{2.1}$$

When integrating over kinematical variables, one obtains

$$\sigma^{\rm DPS}(pp \to c\bar{c}c\bar{c}X) = \frac{1}{2\sigma_{\rm eff}} \sigma^{\rm SPS}(pp \to c\bar{c}X_1) \cdot \sigma^{\rm SPS}(pp \to c\bar{c}X_2). \tag{2.2}$$

These formulas assume that the two parton subprocesses are not correlated with each other. The parameter $\sigma_{\rm eff}$ in the denominator of above formulas can be defined as

$$\sigma_{\rm eff} = \left[\int d^2b (T(\vec{b}))^2 \right]^{-1}, \tag{2.3}$$

where the overlap function

$$T(\vec{b}) = \int f(\vec{b}_1) f(\vec{b}_1 - \vec{b}) d^2b_1, \tag{2.4}$$

if the impact-parameter dependent double-parton distribution functions (dPDFs) are written in the following factorized approximation [7,8]:

$$\Gamma_{i,j}(x_1, x_2; \vec{b}_1, \vec{b}_2; \mu_1^2, \mu_2^2) = F_{i,j}(x_1, x_2; \mu_1^2, \mu_2^2) f(\vec{b}_1) f(\vec{b}_2). \tag{2.5}$$

Without loosing generality, the impact-parameter distribution can be written as

$$\Gamma(b, x_1, x_2; \mu_1^2, \mu_2^2) = F(x_1, \mu_1^2) F(x_2, \mu_2^2) F(b; x_1, x_2, \mu_1^2, \mu_2^2), \tag{2.6}$$

where b is the parton separation in the impact parameter space. In the formula above, the function $F(b; x_1, x_2, \mu_1^2, \mu_2^2)$ contains all information about correlations between the two partons (two gluons in our case). The dependence was studied numerically in Ref. [8] within the Lund Dipole Cascade Model. The biggest discrepancy was found in the small b region, particularly for large μ_1^2 and/or μ_2^2. We shall return to the issue when commenting on our results. To the best of our knowledge, the numerical studies were not applied to any hard process. So, in general, the effective cross section may also depend on many kinematical variables:

$$\sigma_{\rm eff}(x_1, x_2, x_1', x_2', \mu_1^2, \mu_2^2) = \left(\int d^2b F(b; x_1, x_2, \mu_1^2, \mu_2^2) F(b; x_1', x_2', \mu_1^2, \mu_2^2) \right)^{-1}. \tag{2.7}$$

The effect discussed in Ref. [8] may give ~10–20% on an integrated cross section and even more, ~30–50%, in some particular parts of the phase space.

In the present study, we concentrate, rather, on higher-order corrections and ignore the interesting dependence of the impact factors on kinematical variables. The dependence may be different for different dynamical models used.

Gaunt and Stirling [7] also ignored the dependence of the impact factors but included the evolution of the double-parton distribution amplitudes. In our previous paper [2], we have shown that the evolution has a very small impact on the cross section for $pp \to c\bar{c}c\bar{c}X$.

Experimental data from Tevatron [9] provide an estimate of $\sigma_{\rm eff}$ in the denominator of the formula (2.2). Corresponding evaluations from the LHC are expected soon. In our analysis, we take $\sigma_{\rm eff} = 15$ mb. In the most general case, one may expect some violation of this simple factorized Ansatz given by Eq. (2.2) [8].

In the present approach, we concentrate on high energies and, therefore, ignore the quark-induced processes. They could be important only at extremely large pseudorapidities, very large transverse momenta, and huge $c\bar{c}$ invariant masses. In the present analysis, we try to avoid these regions of phase space.

In our present analysis, a cross section for each step is calculated in the k_t-factorization approach; that is,

$$\frac{d\sigma^{\rm SPS}(pp \to c\bar{c}X_1)}{dy_1 dy_2 d^2p_{1,t} d^2p_{2,t}} = \frac{1}{16\pi^2 \hat{s}^2} \int \frac{d^2k_{1t}}{\pi} \frac{d^2k_{2t}}{\pi} \overline{|\mathcal{M}_{g^*g^* \to c\bar{c}}|^2} \times \delta^2(\vec{k}_{1t} + \vec{k}_{2t} - \vec{p}_{1t} - \vec{p}_{2t}) \times \mathcal{F}(x_1, k_{1t}^2, \mu^2) \mathcal{F}(x_2, k_{2t}^2, \mu^2),$$

$$\frac{d\sigma^{\rm SPS}(pp \to c\bar{c}X_2)}{dy_3 dy_4 d^2p_{3,t} d^2p_{4,t}} = \frac{1}{16\pi^2 \hat{s}^2} \int \frac{d^2k_{3t}}{\pi} \frac{d^2k_{4t}}{\pi} \overline{|\mathcal{M}_{g^*g^* \to c\bar{c}}|^2} \times \delta^2(\vec{k}_{3t} + \vec{k}_{4t} - \vec{p}_{3t} - \vec{p}_{4t}) \times \mathcal{F}(x_3, k_{3t}^2, \mu^2) \mathcal{F}(x_4, k_{4t}^2, \mu^2). \tag{2.8}$$

The matrix elements for $g^*g^* \to c\bar{c}$ (off-shell gluons) must be calculated including the transverse momenta of initial gluons as it was done first in Refs. [10–12]. The unintegrated (k_t-dependent) gluon distributions (UGDFs) in the proton are taken from the literature [13–15]. Due to the

emission of soft gluons encoded in these objects, it is believed that a sizeable part of NLO corrections is effectively included. The framework of the k_t-factorization approach is often used with success in describing inclusive spectra of D or B mesons as well as for theoretical predictions for so-called nonphotonic leptons, products of semileptonic decays of charm, and bottom mesons [16–22].

B. Single-parton scattering

The total cross section for the production of the $c\bar{c}c\bar{c}$ final state via single gluon-gluon interaction can be calculated in the parton model approach as

$$\sigma(pp \to c\bar{c}c\bar{c}; W^2) = \int dx_1 dx_2 g(x_1, \mu_F^2) g(x_2, \mu_F^2) \times \sigma(gg \to c\bar{c}c\bar{c}; x_1 x_2 W^2). \quad (2.9)$$

Here, $g(x, \mu^2)$ is integrated (collinear) gluon distribution in a proton (PDF), and W is the proton-proton center-of-mass energy. In practice, the integration is done in $\log_{10} x_1$ and $\log_{10} x_2$, including the corresponding Jacobian transformation. The elementary cross section of Eq. (2.9) enters at $\hat{s} = x_1 x_2 W^2 > 16 m_c^2$. The parton-level cross section in Eq. (2.9) is, therefore, very useful in order to obtain differential distributions in the invariant mass of the $c\bar{c}c\bar{c}$ system.

In the present calculation, we concentrate on LHC energies and consider the $gg \to c\bar{c}c\bar{c}$ subprocesses only. In the high-energy approximation, the elementary cross section can be written in the compact form (see Ref. [4]):

$$d\sigma(gg \to c\bar{c}c\bar{c}) = \frac{N_c^2 - 1}{N_c^2} \frac{4\pi^2 \alpha_s^2}{[\vec{q}^2 + \mu_G^2]^2} I_{g \to c\bar{c}}(z_1, \vec{k}_1, \vec{q}) \times I_{g \to c\bar{c}}(z_2, \vec{k}_2, -\vec{q}) dz_1 \frac{d^2 k_1}{(2\pi)^2} dz_2 \frac{d^2 k_2}{(2\pi)^2} \frac{d^2 q}{(2\pi)^2}. \quad (2.10)$$

Here, the $I_{g \to c\bar{c}}(z_1, \vec{k}_1, \vec{q}_1)$ and $I_{g \to c\bar{c}}(z_2, \vec{k}_2, \vec{q}_2)$ factors, called impact factors, describe the coupling of pairs of $c\bar{c}$ associated with the first and second gluon/proton, respectively. Above z_1 and z_2 are longitudinal momentum fractions of quarks with respect to parent gluons in the first and second pair, respectively, $\vec{k}_i$ are their respective transverse momenta, $\vec{q}$ is exchanged transverse momentum, and μ_G is gluon mass that can be put to zero at least mathematically. At low energies, this formula must be corrected for threshold effects [4]. The differential cross sections for $pp \to c\bar{c}c\bar{c}X$ can be obtained by replacing the $\sigma(gg \to c\bar{c}c\bar{c})$ by $d\sigma(gg \to c\bar{c}c\bar{c})$ in Eq. (2.9). Details about how the arguments of α_s are chosen are discussed in Ref. [4].

Our approach includes subprocesses coherently to be contrasted to Ref. [6], in which they were separated one from each other to simplify calculations. In addition, we get a practical agreement with results of calculations in Ref. [23].

C. Double meson production

Kinematical correlations between quarks and antiquarks are not accessible experimentally. Instead, one can measure correlations between heavy mesons or nonphotonic electrons. In this paper, we will analyze kinematical correlations between charmed mesons. In particular, we are interested in correlations between D_i and D_j mesons (both containing c quarks) or between $\bar{D}_i$ and $\bar{D}_j$ mesons (both containing $\bar{c}$ antiquarks). In order to calculate correlations between mesons, we follow here the fragmentation function technique for the hadronization process:

$$\frac{d\sigma(pp \to DDX)}{dy_1 dy_2 d^2 p_{1,t}^D d^2 p_{2,t}^D} \approx \int \frac{D_{c \to D}(z_1)}{z_1} \cdot \frac{D_{c \to D}(z_2)}{z_2} \cdot \frac{d\sigma(pp \to ccX)}{dy_1 dy_2 d^2 p_{1,t}^c d^2 p_{2,t}^c} dz_1 dz_2, \quad (2.11)$$

where $p_{1,t}^c = \frac{p_{1,t}^D}{z_1}$, $p_{2,t}^c = \frac{p_{2,t}^D}{z_2}$ and meson longitudinal fractions $z_1, z_2 \in (0, 1)$. We have made an approximation assuming that y_1, y_2 and ϕ are unchanged in the fragmentation process. The multidimensional distribution for both c quarks (or both $\bar{c}$ antiquarks) is convoluted with fragmentation functions simultaneously for each of the two quarks (or each of the two antiquarks). As a result of the hadronization, one obtains corresponding two-meson multidimensional distribution. In the last step, experimental kinematical cuts on the distributions can be imposed. Then, the resulting distributions can be compared with experimental ones. For numerical calculations here, we apply the Peterson fragmentation function, often used in the case of heavy quarks [24]. We have shown in Ref. [5] that this scheme works very well in the case of inclusive D^0 meson spectra as well as for $D^0 \bar{D}^0$ kinematical correlations.

III. RESULTS

A. Parton level

We start from inclusive distributions of charm quarks (or antiquarks). As discussed in Ref. [5], the standard single-parton scattering contribution to $pp \to c\bar{c}X$ seems insufficient to describe inclusive spectra of charmed mesons as measured by the ATLAS, ALICE, and the LHCb collaborations [25–27]. The $c\bar{c}c\bar{c}$ production also contributes to the inclusive charm production. In Fig. 1, we show such a contribution to transverse momentum distribution (left panel) and rapidity distribution (right panel) together with a theoretical uncertainty band. In this calculation, the Kimber-Martin-Ryskin (KMR) UGDF [13] was used with the Martin-Stirling-Thorne-Watt (MSTW08) [28] collinear gluon PDF. The solid line corresponds to the central value

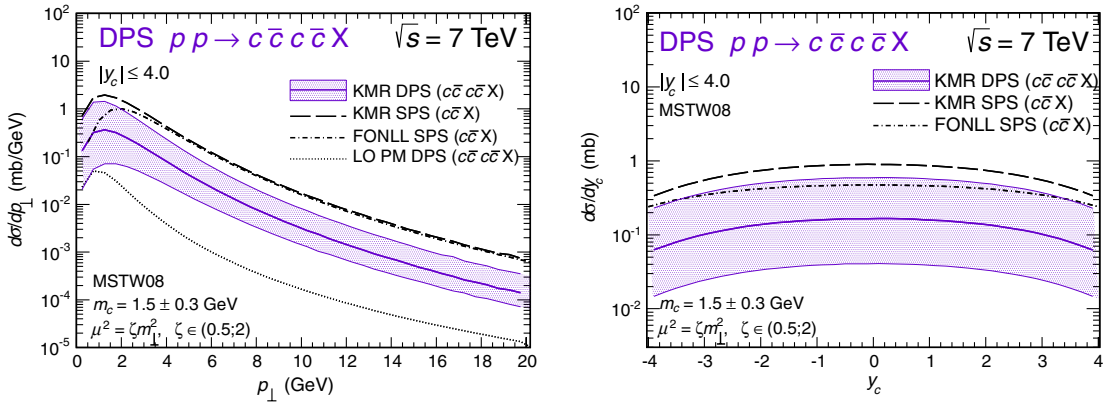

FIG. 1 (color online). Transverse momentum (left) and rapidity (right) of charm quarks from SPS $c\bar{c}$ (long-dashed line) and DPS $c\bar{c}c\bar{c}$ (solid line with shaded band) production. In this calculation, the KMR UGDF was used, and the factorization scale and quark mass for the DPS contribution were varied as explained in the figure. For comparison, LO collinear DPS distribution (dotted line) and the FONLL SPS $c\bar{c}$ result (dashed-dotted line) are shown.

of our predictions. The uncertainties are obtained by changing charm quark mass $m_c = 1.5 \pm 0.3$ GeV, which, in general, is not well-known, and by varying renormalization and factorization scales $\mu^2 = \mu_R^2 = \mu_F^2 = \zeta m_\perp^2$, where $\zeta \in (0.5; 2)$. The shaded bands represent both these sources of uncertainties summed in quadrature. As a reference point, we plot the contribution from standard single-scattering $c\bar{c}$ production, obtained in the k_t-factorization approach (long-dashed line) as well as calculated with the help of the FONLL code [29] (dashed-dotted line). As can be seen, both of these models are consistent and give very similar numerical results for transverse momenta $p_t > 3$ GeV. The agreement at larger transverse momenta suggests that, in the case of charm quark production, the k_t-factorization approach with the KMR UGDFs very well reproduces NLO corrections. These aspects of $c\bar{c}$ production were discussed in more detail in Ref. [5]. The region of small transverse momenta of quarks is sensitive to extrapolation of perturbative QCD UGDF to a nonperturbative region of small gluon transverse momenta.

Since the DPS uncertainty band is very broad, it becomes clear that this contribution is quite sizeable and must be included in the total balance of charm quark (antiquark) production. For comparison, we also show the DPS result obtained previously in Ref. [2] in the LO collinear approach. It is much smaller than the k_t-factorization result, especially at larger transverse momenta.

In Fig. 2, we compare the DPS results for the transverse momentum (left panel) and rapidity (right panel) distributions obtained with different UGDFs from the literature [13–15]. The KMR UGDF gives the largest cross section. Numerical results of DPS are more sensitive to the choice of UGDFs than in the case of SPS $c\bar{c}$ production, which can be understood by a different power of UGDFs in the cross section formula (fourth in DPS $c\bar{c}c\bar{c}$ vs second in SPS $c\bar{c}$). We also use here the Kwieciński-Martin-Staśto (KMS) [14] and Jung set$A+$ [15] parametrizations. In turn, in Fig. 3, we confront theoretical uncertainties of SPS single-pair ($c\bar{c}$) and DPS two-pair ($c\bar{c}c\bar{c}$) production. Again, uncertainty of the two-pair production is much larger than that for single-pair production.

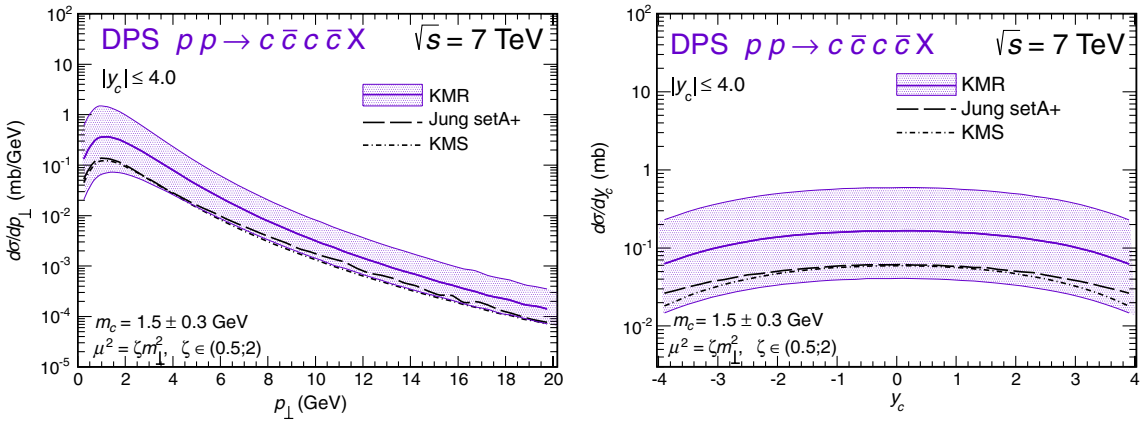

FIG. 2 (color online). Transverse momentum (left) and rapidity (right) distributions of charm quarks produced in DPS $c\bar{c}c\bar{c}$ production for different unintegrated gluon distributions.

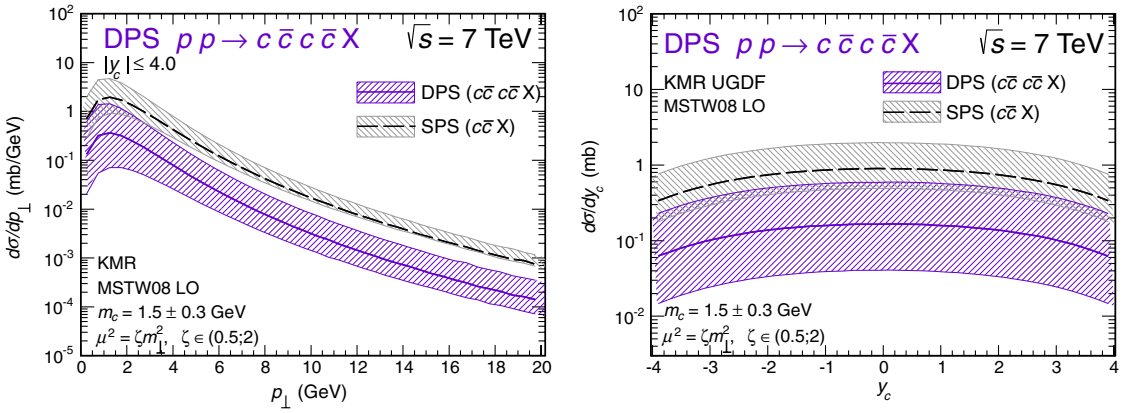

FIG. 3 (color online). Comparison of the SPS $c\bar{c}$ and DPS $c\bar{c}c\bar{c}$ contributions to the inclusive charm quark (antiquark) production together with theoretical uncertainties due to the choice of scales and those related with quark mass (summed in quadrature).

In Ref. [2], we have proposed several correlation distributions to be studied in order to identify the DPS effects. Here, we present the same distributions as in Ref. [2] but within the k_t-factorization approach. In Fig. 4, we show distributions in invariant mass $M_{c\bar{c}}$ (left panel) and the rapidity difference of quarks/antiquarks $Y_{\rm diff} = y_c - y_{\bar{c}}$ (right panel) from the same scattering ($c_1\bar{c}_2$ or $c_3\bar{c}_4$) and from different scatterings ($c_1\bar{c}_4$ or $c_3\bar{c}_2$ or c_1c_3 or $\bar{c}_2\bar{c}_4$) for various UGDFs specified in the figure. The shapes of distributions in the figure are almost identical as their counterparts obtained in the LO collinear approach in Ref. [2].

In Fig. 5, we show distributions in an azimuthal angle difference between quarks/antiquarks $\varphi_{c\bar{c}}$ from the same and from different scatterings. While, in the case of the same scattering, distribution strongly depends on the choice of UGDF, the quarks/antiquarks from different scattering are not correlated, which is inherent property of the simple factorized model. Our distinguishing of scatterings can be done only in the model calculation. Experimentally, one observes both types together after hadronization, which naturally may bring additional decorrelation.

Finally, in Fig. 6, we present distribution in the transverse momentum of the pair of quarks $p_\perp^{c\bar{c}}$. In the LO collinear approach, the distribution for emission in the same scattering is very different from the case of emissions from different scatterings [2]. The picture in the k_t-factorization approach is, however, very different. The respective distributions for the same and different scatterings are rather similar. This means that the transverse momentum of the pair may not be the best quantity use in order to identify the DPS effects.

B. Meson level

Production of two pairs of $c\bar{c}$ on the partonic level leads to the situations that very often two mesons, both containing c quarks or/and both containing $\bar{c}$ antiquarks, are produced on the hadronic level in one event. Therefore, the presence of two such mesons may be considered as a signal of production of $c\bar{c}c\bar{c}$ on the partonic level. Recently, the LHCb Collaboration performed a first measurement of $D_iD_j + \bar{D}_i\bar{D}_j$ production in the fiducial range of the detector acceptance $2 < y_D < 4$ and $3 < p_\perp^D < 12$ GeV [3].

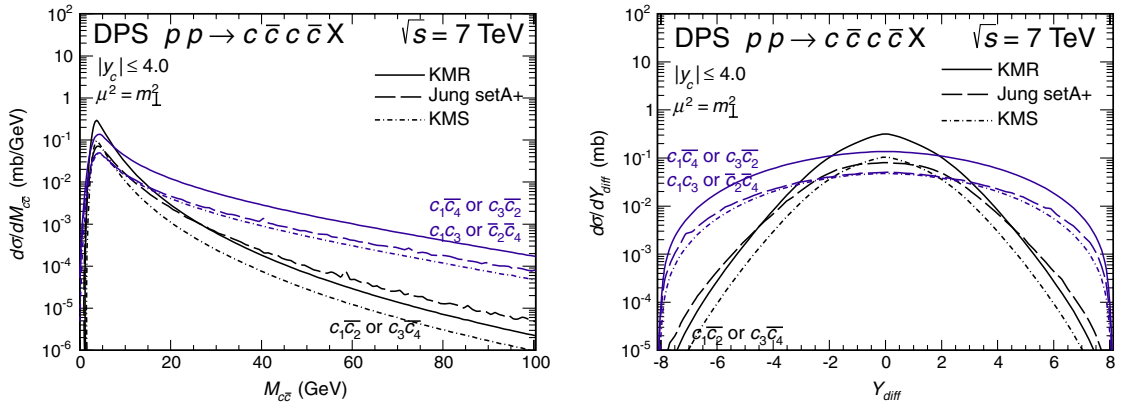

FIG. 4 (color online). Distribution in the invariant mass of quark/antiquark $M_{c\bar{c}}$ (left) and distribution in the rapidity distance between quarks/antiquarks $Y_{\rm diff}$ (right) from the same ($c_1\bar{c}_2$ or $c_3\bar{c}_4$) and from different scatterings ($c_1\bar{c}_4$ or $c_3\bar{c}_2$ or c_1c_3 or $\bar{c}_2\bar{c}_4$), calculated with different UGDFs.

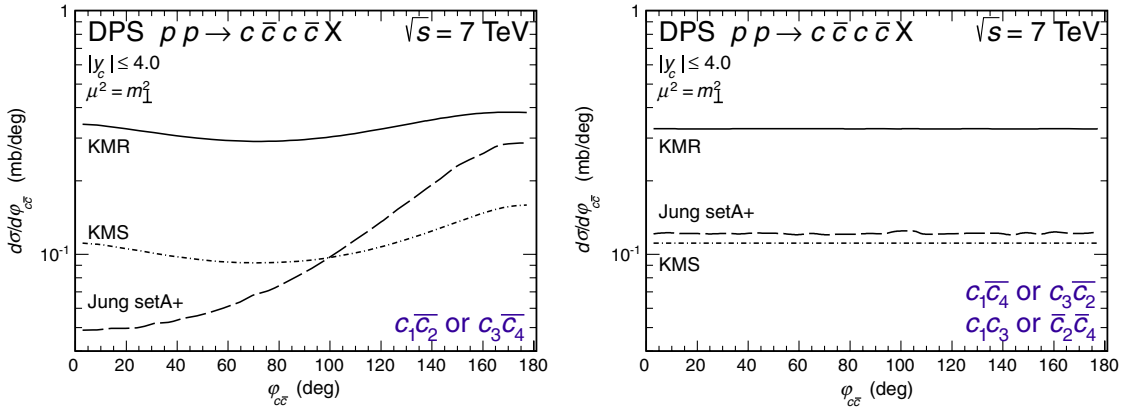

FIG. 5 (color online). Distribution in an azimuthal angle $\varphi_{c\bar{c}}$ between quarks/antiquarks from the same scattering (left) and from different scatterings (right), calculated with different UGDFs.

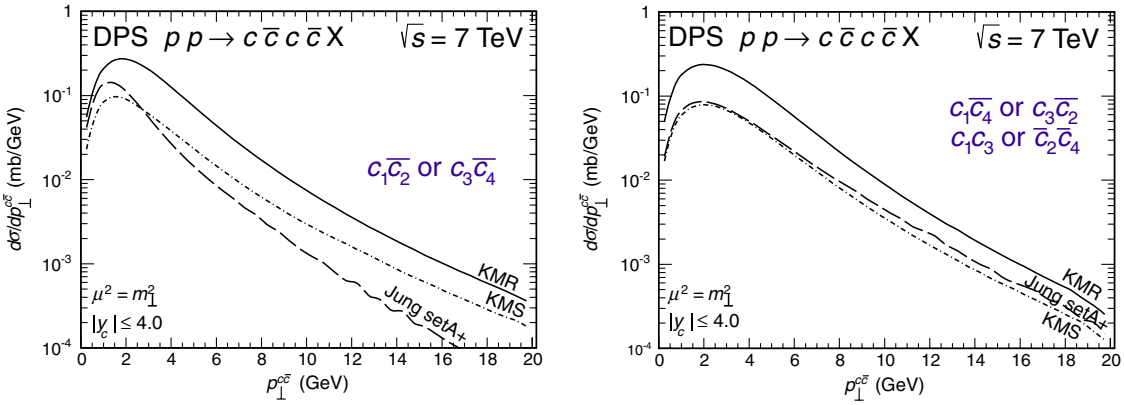

FIG. 6 (color online). Distribution in transverse momentum of the quark/antiquark pair $p_\perp^{c\bar{c}}$ from the same scattering (left) and from different scatterings (right), calculated with different UGDFs.

As described in Sec. II, we have prepared a code that keeps track of full kinematical information about each of both quarks or both antiquarks and similar information about both mesons. Such a multidimensional map is used then to impose adequate experimental cuts.

In Table I, we have collected DPS cross sections for different pairs of mesons relevant for considered kinematics obtained with different unintegrated gluon distributions. As was shown in Ref. [5], theoretical predictions for the production of charmed meson pairs in the LHCb kinematics are very sensitive to the value of ε_c parameter in the Peterson fragmentation function. There, rather harder functions (with smaller ε_c) are suggested for a better description of the experimental data, which is also

TABLE I. Total cross sections for meson-meson pair production for three different UGDFs.

		$\sigma_{\rm tot}^{\rm THEORY}$ [nb]					
		KMR $^{+}_{-}(\mu)$ $^{+}_{-}(m_c)$		Jung setA+		KMS	
Mode	$\sigma_{\rm tot}^{\rm EXP}$ [nb]	$\varepsilon_c = 0.05$	$\varepsilon_c = 0.02$	$\varepsilon_c = 0.05$	$\varepsilon_c = 0.02$	$\varepsilon_c = 0.05$	$\varepsilon_c = 0.02$
D^0D^0	$690 \pm 40 \pm 70$	$265\ ^{+140}_{-77}\ ^{+157}_{-94}$	400	120	175	84	126
D^0D^+	$520 \pm 80 \pm 70$	$212\ ^{+112}_{-62}\ ^{+126}_{-75}$	319	96	140	67	100
$D^0D_S^+$	$270 \pm 50 \pm 40$	$75\ ^{+40}_{-22}\ ^{+45}_{-27}$	113	34	50	24	36
D^+D^+	$80 \pm 10 \pm 10$	$42\ ^{+23}_{-13}\ ^{+26}_{-15}$	64	19	28	13	20
$D^+D_S^+$	$70 \pm 15 \pm 10$	$30\ ^{+16}_{-9}\ ^{+18}_{-11}$	45	14	20	10	14
$D_S^+D_S^+$	$\cdots$	$11\ ^{+5}_{-3}\ ^{+6}_{-4}$	16	5	7	3	5

in agreement with observations made in the FONLL framework [30,31]. Therefore, we present results for two different values of the ε_c parameter. Here, we have added together cross sections for charge-conjugated channels: $\sigma_{D_iD_j} + \sigma_{\bar{D}_i\bar{D}_j}$. The calculated cross sections are somewhat smaller than the experimental ones. Only the upper limit of our predictions with the Kimber-Martin-Ryskin UGDF and with $\varepsilon_c = 0.02$ in the Peterson fragmentation function gives results that are close to the experimental data, given the uncertainties on the choice of the factorization/renormalization scale and on the charm quark mass.

So far, we have considered only DPS contribution to D_iD_j (or $\bar{D}_i\bar{D}_j$) production. In Fig. 7, we show in addition corresponding SPS contribution. The SPS contribution to the transverse momentum distribution (left panel) is more than 2 orders of magnitude smaller than the DPS one. For the rapidity distribution (right panel), the difference is only 1 order of magnitude. This effect is slightly unintuitive. However, it can be understood by a comparison of the two-dimensional distributions in the rapidity of one and the second D meson for DPS and SPS production (see Fig. 8).

In the case of DPS, the two mesons are not correlated (in this plane), in contrast to the SPS mechanism, in which they are strongly anticorrelated. When one meson is produced in the forward rapidity region, the second is preferentially produced in the backward rapidity region, or vice versa. One can also conclude that, in the case of D_iD_j ($\bar{D}_i\bar{D}_j$) pair production, the specific LHCb kinematical range leads to a dumping of the SPS cross section. The requirement that both D mesons have to reach the detector makes the SPS contribution almost negligible. Quite different conclusions can be drawn in the case of inclusive D meson measurements.

In the present paper, we have calculated SPS $c\bar{c}c\bar{c}$ contribution in the high-energy approximation, which may not be the best approximation for the LHCb kinematics for which the distance between both c or both $\bar{c}$ is rather small. Therefore, to draw definite conclusions, future studies of the $pp \to c\bar{c}c\bar{c}X$ process are needed, and they must include a complete set of diagrams for the SPS $c\bar{c}c\bar{c}$ mechanism. Furthermore, if the improved calculations of the SPS mechanism will not provide a somewhat better

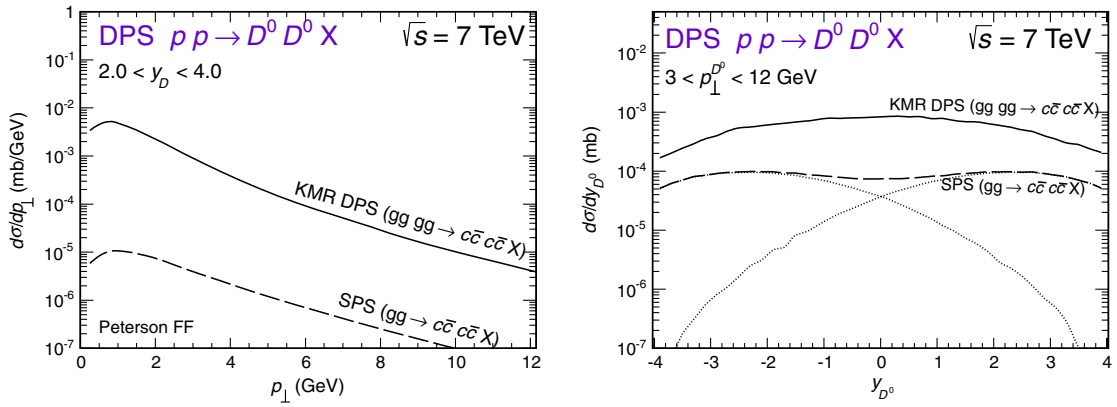

FIG. 7 (color online). Distributions in transverse momentum (left panel) and rapidity (right panel) of a single D^0 meson from the D^0D^0 pair events. The solid lines correspond to the DPS mechanism, and the long-dashed lines represent contributions from SPS production of D^0D^0 pairs. Here, we impose kinematical cuts adequate for the LHCb kinematics.

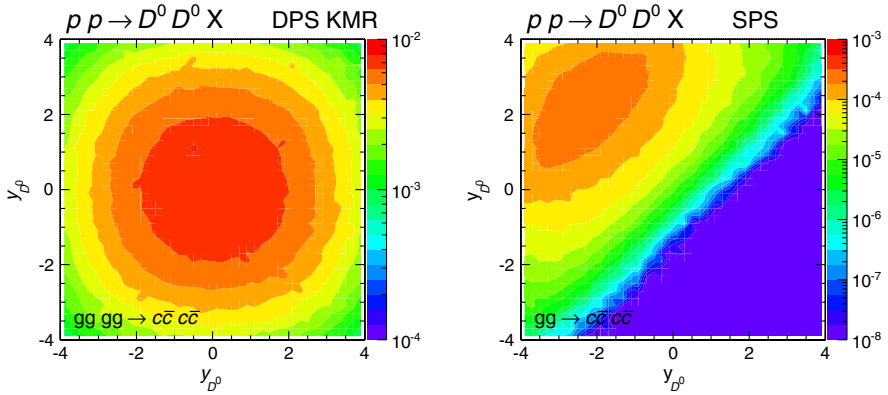

FIG. 8 (color online). Two-dimensional distributions in rapidity of one D^0 meson and rapidity of the second D^0 meson for DPS (left) and SPS (right).

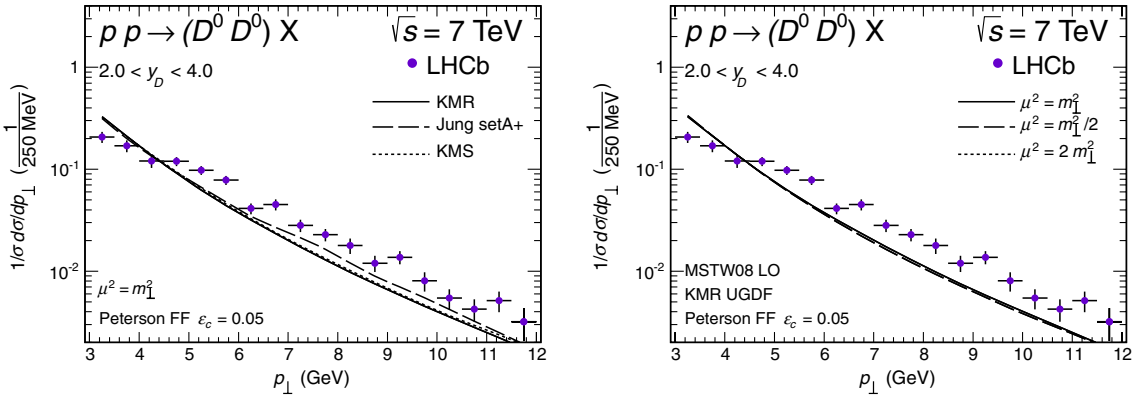

FIG. 9 (color online). Transverse momentum distribution of D^0 mesons from the D^0D^0 pair contained in the LHCb kinematical region. The left panel shows dependence on UGDFs, while the right panel illustrates dependence of the result for the KMR UGDF on the factorization/renormalization scales. The MSTW08 collinear distribution was used to generate KMR UGDF.

description of the total cross sections measured by the LHCb, one has to look for other mechanisms that can contribute and fill the predicted missing strength.

The LHCb Collaboration presented also several differential distributions for the simultaneous production of two DD and $\bar{D}\,\bar{D}$ mesons. Here, we consider only examples for the D^0D^0 (identical to $\bar{D}^0\bar{D}^0$) channel.

In Fig. 9, we present distribution in transverse momentum of one of the D^0 mesons, provided that both are measured within the LHCb experiment coverage specified in the figure caption. Our theoretical distributions have shapes in rough agreement with the experimental data. The shapes of the distributions are almost identical for different UGDFs used in the calculations (left panel) and are independent on the choice of scales in the case of the KMR model (right panel).

In Fig. 10, we show distribution in the D^0D^0 invariant mass $M_{D^0D^0}$ for both D^0's measured in the kinematical region covered by the LHCb experiment. Here, the shapes of the distributions have the same behavior for various UGDFs and are insensitive to changes of scales as in the previous figure. The characteristic minimum at small invariant masses is a consequence of experimental cuts (see Ref. [5]) and is rather well-reproduced. Our approach fails at large dimeson invariant masses. The large $M_{D^0D^0}$ invariant masses are probably correlated to large scales $\mu^2_{1/2}$ and/or $\mu^2_{3/4}$. If that can be related to the effects of factorization violation discussed in Ref. [8] requires further studies.

Finally, in Fig. 11, we show distribution in an azimuthal angle $\varphi_{D^0D^0}$ between both D^0's. While the theoretical DPS contribution is independent of the relative azimuthal angle, there is some small residual dependence on the azimuthal angle in experimental distribution. This may show that there is some missing mechanism that gives contributions both at small and large $\Delta\varphi$. However, this discrepancy may be also an inherent property of the DPS factorized model that does not allow for any azimuthal correlations between particles produced in different hard scatterings. We wish to emphasize in this context that the angular azimuthal correlation patterns for $D^0\bar{D}^0$, discussed in Ref. [5], and for D^0D^0 ($\bar{D}^0\,\bar{D}^0$), discussed here, are quite different. The

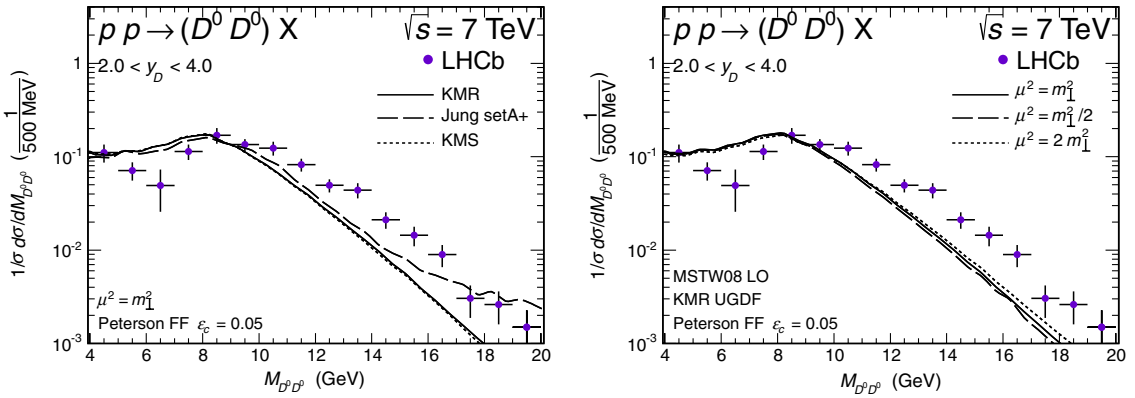

FIG. 10 (color online). $M_{D^0D^0}$ invariant mass distribution for D^0D^0 contained in the LHCb kinematical region. The left panel shows dependence on UGDFs, while the right panel illustrates dependence of the result for the KMR UGDF on the factorization/renormalization scales.

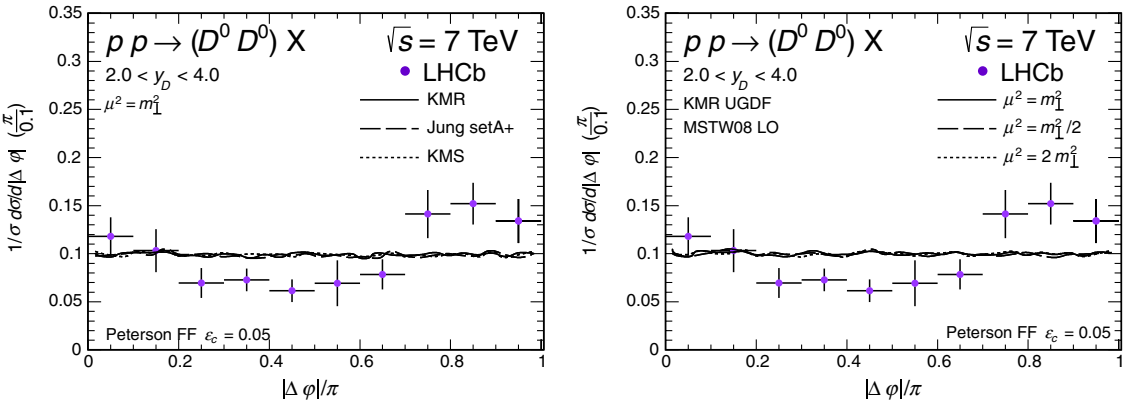

FIG. 11 (color online). Distribution in the azimuthal angle $\varphi_{D^0D^0}$ between both D^0's. The left panel shows dependence on UGDFs, while the right panel illustrates dependence of the result for the KMR UGDF on the factorization/renormalization scales.

distribution for D^0D^0 ($\bar{D}^0\bar{D}^0$) is much flatter compared to the $D^0\bar{D}^0$ one that shows a pronounced maximum at $\varphi_{D^0\bar{D}^0} = 180°$ (mostly from pair creation) and $\varphi_{D^0\bar{D}^0} = 0°$ (mostly from gluon splitting) [5]. This qualitative difference is, in our opinion, a model-independent proof of the dominance of DPS effects in the production of D^0D^0 ($\bar{D}^0\bar{D}^0$).

C. DPS $c\bar{c}c\bar{c}$ production and inclusive charmed meson distributions

Since the DPS cross section is very large, it is also very important to look at the DPS $c\bar{c}c\bar{c}$ contribution to inclusive charmed meson spectra. Let us consider, for example, transverse momentum distribution of a charmed D_i meson. The corresponding DPS $c\bar{c}c\bar{c}$ contribution can be written as

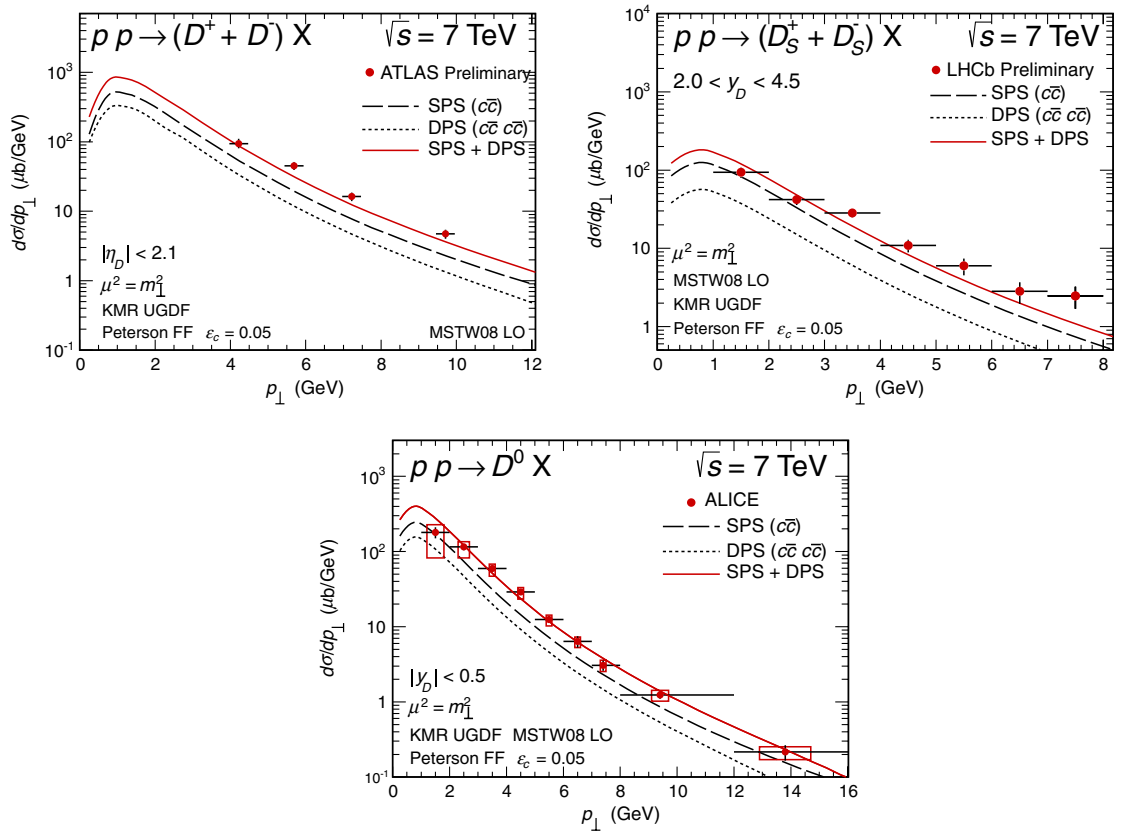

FIG. 12 (color online). Inclusive transverse momentum distributions of different charmed mesons measured by different groups at the LHC. The long-dashed line corresponds to the standard SPS $c\bar{c}$ production, and the dotted line represents the DPS $c\bar{c}c\bar{c}$ contribution.

$$\frac{d\sigma_{\rm inc}^{D_i,\rm DPS}}{dp_t} = P_{D_i}(1-P_{D_i})\frac{d\sigma^D}{dp_{1,t}}\Big|_{p_{1,t}=p_t}(-2.1<\eta_1<2.1, -\infty<\eta_2<\infty)$$
$$+ P_{D_i}(1-P_{D_i})\frac{d\sigma^D}{dp_{2,t}}\Big|_{p_{2,t}=p_t}(-\infty<\eta_1<\infty, -2.1<\eta_2<2.1)$$
$$+ P_{D_i}P_{D_i}\frac{d\sigma^D}{dp_{1,t}}\Big|_{p_{1,t}=p_t}(-2.1<\eta_1<2.1, -\infty<\eta_2<\infty)$$
$$+ P_{D_i}P_{D_i}\frac{d\sigma^D}{dp_{2,t}}\Big|_{p_{2,t}=p_t}(-\infty<\eta_1<\infty, -2.1<\eta_2<2.1). \quad (3.1)$$

In the formula above, P_{D_i} is a shorthand notation for the branching fraction $P_{c\to D_i}$, and σ^D is the cross section for D mesons, assuming artificially the branching fraction equal to 1. The formula above can be somewhat simplified when combining similar terms.

In Fig. 12, we show inclusive one-pair (long-dashed line) contribution, inclusive DPS two-pair contribution (dotted line), and the sum of both terms to transverse momentum distribution of different D mesons (solid line). The DPS $c\bar{c}c\bar{c}$ contribution is of the same order as the standard traditional SPS $c\bar{c}$ contribution. This is a completely new situation compared to what it was at smaller energies. The sum of both contributions almost describes the different experimental data. As discussed in the previous section, the SPS $c\bar{c}c\bar{c}$ contribution can be of the order of 10% of the DPS $c\bar{c}c\bar{c}$ contribution. At higher energies, one could expect even relatively larger DPS $c\bar{c}c\bar{c}$ contribution. A problem could start, however, that then one enters the region of really small gluon longitudinal momentum fractions $x<10^{-4}$ for which the gluon UGDFs (or PDFs) are not well-known. In this case, realistic models of UGDFs are badly needed. Do we have such a distribution at present?

As discussed in our earlier analysis [5], the uncertainty of the SPS contributions is not sufficient to understand the inclusive spectra. In addition, ignoring the DPS contribution here would mean a complete failure for correlation observables discussed above.

IV. CONCLUSIONS

In this paper, we have discussed production of $c\bar{c}c\bar{c}$ in the double-parton scattering and single-parton scattering in the $gg\to c\bar{c}c\bar{c}$ subprocess. The double-parton scattering is calculated in the factorized ansatz with each step calculated in the k_t-factorization approach, i.e., including effectively higher-order QCD corrections.

The cross section in the k_t-factorization approach turned out to be much larger than its counterpart calculated in the LO collinear approach. The distribution in rapidity difference between quarks/antiquarks from the same and different scatterings turned out to have a similar shape as in the LO collinear approach. The same is true for invariant masses of pairs of quark-quark, antiquark-antiquark, quark-antiquark, etc. The distribution in the transverse momentum of the pair from the same scattering turned out to be similar to that for the pairs originating from different scatterings.

We have also calculated cross sections for the production of D_iD_j (both containing the c quark) and $\bar{D}_i\bar{D}_j$ (both containing the $\bar{c}$ antiquark) pairs of mesons. The results of the calculation have been compared to recent results of the LHCb Collaboration.

The total rates of the meson pair production depend on the unintegrated gluon distributions. The best agreement with the LHCb result has been obtained for the Kimber-Martin-Ryskin UGDF. This approach as discussed already in the literature effectively includes higher-order QCD corrections.

As an example, we have also calculated several differential distributions for D^0D^0 pair production. Rather good agreement has been obtained for the transverse momentum distribution of D^0 ($\bar{D}^0$) mesons and D^0D^0 invariant mass distribution. The distribution in the azimuthal angle between both D^0's suggests that some contributions may be still missing. The single parton scattering contribution, calculated in the high-energy approximation, turned out to be rather small. This should be checked in exact $2\to 4$ parton model calculations in the future.

We have shown that the DPS mechanism of $c\bar{c}c\bar{c}$ production gives a new significant contribution to inclusive charmed meson spectra. For instance, the description of the inclusive ATLAS, ALICE, and LHCb data is very difficult in terms of the conventional SPS ($c\bar{c}$) contribution [5].

Since we have shown that the DPS mechanism gives significant contribution to the inclusive spectra of charmed mesons, the estimate of DPS effects, presented in Ref. [6] and based on the experimental inclusive cross section, leads to an overestimation of the DPS effect. The estimation of Ref. [6] implicitly assumes no DPS contribution to the inclusive spectra.

Summarizing, the present study of $c\bar{c}c\bar{c}$ reaction in the k_t-factorization approach has shown that this reaction is an extremely good testing ground of double-parton scattering effects. The LHCb kinematics is not the best in this respect. Both ATLAS and CMS collaborations could measure the production of pairs of D_iD_j and/or $\bar{D}_i\bar{D}_j$

mesons with large rapidity distance where the DPS mechanism is predicted to clearly dominate over the SPS mechanism. Another potentially interesting place to investigate the DPS effect is the $pp \to J/\psi J/\psi X$ reaction [32]. Similarly, as for $pp \to c\bar{c}c\bar{c}X$ discussed here, the large rapidity gap between two J/ψ's should select clear sample of DPS mechanism.

ACKNOWLEDGMENTS

The authors thank Ivan Belyaev and Marek Szczekowski for useful discussions of many aspects of the LHCb experimental data and Wolfgang Schäfer for discussion of the single-parton scattering contribution. This work is supported in part by the Polish Grant Nos. DEC-2011/01/B/ST2/04535 and No. N202 237040.

[1] P. Bartalini *et al.*, arXiv:1111.0469; Report No. ANL-HEP-PR-11-65; Report No. CMS-CR-2011-048; Report No. DESY 11-185.
[2] M. Łuszczak, R. Maciuła, and A. Szczurek, Phys. Rev. D **85**, 094034 (2012).
[3] R. Aaij *et al.* (The LHCb collaboration), J. High Energy Phys. 06 (2012) 141.
[4] W. Schäfer and A. Szczurek, Phys. Rev. D **85**, 094029 (2012).
[5] R. Maciuła and A. Szczurek, arXiv:1301.3033.
[6] A. V. Berezhnoy, A. K. Likhoded, A. V. Luchinsky, and A. A. Novoselov, Phys. Rev. D **86**, 034017 (2012).
[7] J. R. Gaunt and W. J. Stirling, J. High Energy Phys. 03 (2010) 005.
[8] C. Flensburg, G. Gustafson, L. Lönnblad, and A. Ster, J. High Energy Phys. 06 (2011) 066.
[9] F. Abe *et al.* (CDF Collaboration), Phys. Rev. D **56**, 3811 (1997); Phys. Rev. Lett. **79**, 584 (1997).
[10] S. Catani, M. Ciafaloni, and F. Hautmann, Nucl. Phys. **366**, 135 (1991).
[11] J. C. Collins and R. K. Ellis, Nucl. Phys. **B360**, 3 (1991).
[12] R. D. Ball and R. K. Ellis, J. High Energy Phys. 05 (2001) 053.
[13] M. A. Kimber, A. D. Martin, and M. G. Ryskin, Phys. Rev. D **63**, 114027 (2001).
[14] J. Kwieciński, A. D. Martin, and A. M. Staśto, Phys. Rev. D **56**, 3991 (1997).
[15] H. Jung and G. P. Salam, Eur. Phys. J. C **19**, 351 (2001); H. Jung, arXiv:hep-ph/0411287.
[16] Ph. Hägler, R. Kirschner, A. Schäfer, I. Szymanowski, and O. V. Teryaev, Phys. Rev. D **62**, 071502 (2000).
[17] S. P. Baranov and M. Smizanska, Phys. Rev. D **62**, 014012 (2000).
[18] S. P. Baranov, A. V. Lipatov, and N. P. Zotov, Yad. Fiz. **67**, 859 (2004) [Phys. At. Nucl. **67**, 837 (2004)].
[19] Yu. M. Shabelski and A. G. Shuvaev, Phys. At. Nucl. **69**, 314 (2006).
[20] M. Łuszczak, R. Maciuła, and A. Szczurek, Phys. Rev. D **79**, 034009 (2009).
[21] R. Maciuła, A. Szczurek, and G. Ślipek, Phys. Rev. D **83**, 054014 (2011).
[22] H. Jung, M. Kraemer, A. V. Lipatov, and N. P. Zotov, Phys. Rev. D **85**, 034035 (2012); J. High Energy Phys. 01 (2011) 085.
[23] V. D. Barger, A. L. Stange, and R. J. N. Phillips, Phys. Rev. D **44**, 1987 (1991).
[24] C. Peterson, D. Schlatter, I. Schmitt, and P. M. Zerwas, Phys. Rev. D **27**, 105 (1983).
[25] ATLAS Collaboration, Report No. ATLAS-CONF-2011-017.
[26] B. Abelev *et al.* (The ALICE collaboration), J. High Energy Phys. 01 (2012) 128.
[27] LHCb Collaboration, Report No. LHCb-CONF-2010-013.
[28] A. D. Martin, W. J. Stirling, R. S. Thorne, and G. Watt, Eur. Phys. J. C **63**, 189 (2009); **64**, 653 (2009).
[29] M. Cacciari, M. Greco, and P. Nason, J. High Energy Phys. 05 (1998) 007; M. Cacciari, S. Frixione, and P. Nason, J. High Energy Phys. 03 (2001) 006.
[30] M. Cacciari, P. Nason, and R. Vogt, Phys. Rev. Lett. **95**, 122001 (2005).
[31] M. Cacciari, S. Frixione, N. Houdeau, M. L. Mangano, P. Nason, and G. Ridolfi, J. High Energy Phys. 10 (2012) 137.
[32] S. P. Baranov, A. M. Snigirev, N. P. Zotov, A. Szczurek, and W. Schäfer, Phys. Rev. D **87**, 034035 (2013).